

CRITICAL STATE OF A WHEEL WORKING SURFACE

Petrov S.V., Markashova L.I.¹, Valevich M.L.², Karpinos B. S.², Barilo V. G.³

Abstract

This work was aimed at development of a technology and equipment for plasma surface hardening to provide an increase in contact-fatigue strength of metal and, as a result, an increase in service life of the wheelsets. During operation the working surface of a wheel is affected by a combination of different loads. It is an established fact that the working surface layer of a wheel material may lose almost all its ability to resist fracture under the simultaneous effect of the operating factors. This shows up as a complete loss of ductility, embrittlement, and formation of a surface crack network looking like a fish scale, whereas at the level of a fine structure this results in accumulation of defects and disordering. When such microcracks get into the unfavourable field of the first-order tensile stresses, they may lead to fracture of the shroud. Such fractures can be justifiably classed with unexpected ones, having a deeply "concealed" real cause. The authors conducted analysis of structure and physical-mechanical properties of the subsurface layers formed under the effect of different factors in wheel steel in the zone of contact with the rail. The purpose of this study was to reveal the prime causes of fracture of a wheel under the simultaneous effect of the operating factors.

Keywords: wheelsets, plasma, hardening, wear, reliability, microcracks

HEAT HARDENING OF WHEELSETS

Wear of wheels and rails is a complex process, depending upon many factors, which are interrelated in the quantitative respect. Method of plasma surface hardening is among the cheapest and most efficient methods used at repair enterprises to increase wear resistance of roll surfaces, including the flange [1]. The purpose of plasma surface hardening of the wheelsets is to increase their life and improve reliability in operation without any sacrifice of performance of rails. To achieve this purpose, it is necessary to solve three inter-related and conflicting problems [2].

- The first of them consists in providing local hardening of the working surface of a flange to achieve the preset value of hardness and finely dispersed structure of metal of the hardened layer. It is these factors that ensure a

¹ The E.O.Paton Electric Welding Institute of the National Academy of Sciences of Ukraine, 11 Bozhenko str., Kyiv, Ukraine, 03680

² G.S. Pisarenko Institute for Problems of Strength of the National Academy of Sciences of Ukraine
2, Timiryazevskaya Str., Kyiv, Ukraine, 01014

decrease in the rates of wear of flanges and the coefficient of friction between the flange and side surface of the rail head, which has a favourable effect on rails, especially in curves, through delaying their wear.

- The second problem is associated with the formation of fields of internal stresses acting both in the bulk of metal and between grains. Rapid heating and cooling of a local region of the massive wheel lead to structural transformations, which involve changes in the specific volume, and to plastic deformations, i.e. compression and tension. The most serious problems arise in hardening of tyres. Material of the wheel tyre is in a complex heterogeneous stressed state.

- The third problem is associated with a change in a fine structure of metal caused by plasma surface heating [3]. Depending upon the plasma hardening conditions the results obtained may be quite opposite. In a case of the proper technology, the resulting metal structure will be mostly of the troostite-sorbite and fine-laminated type mixed with structureless martensite. This structure has a somewhat increased microhardness and is characterized by the absence of nonmetallic inclusions, of the sulphide type in particular. The resulting fine structure contains dispersed sub-structural elements (sub-grains, blocks, cells) and features a uniform distribution of dislocations without dislocation density gradients. In this case the initial metal structure and all mechanical properties are improved. In a case of violation of the technology the structure is coarse-laminated (ferritic-pearlitic), containing ferritic fringes and nonmetallic inclusions of the sulphide type. The coarser sub-structure with a non-uniform distribution of dislocations and dramatic dislocation density gradients are formed as a rule in a region of contact of rigid and soft structural constituents (cement laminae with ferritic interlayers in pearlite or at the pearlite grain boundaries with ferritic fringes, etc.). In this case there is a risk of cracking

The technology of plasma surface hardening of TOPAS Ltd. is characterized by new capabilities in terms of increasing contact-fatigue strength and, therefore, increasing reliability of traction for wheelsets. Intensity of wear of the wheelset flanges after plasma hardening is much lower than that of the traditionally treated ones (2.5-3 times). The technology have been developed for hardening of the wheelsets has two peculiar features: 1. Local (within the zone of the highest wear) surface hardening of the wheel flange to a depth of 2.5-3 mm and width of 35 mm, ensuring an increase in hardness from 280 HB (in the base metal) to 450 HB. This provides an optimal relationship in hardness of the wheel and rail surfaces in contact; 2) Change in structure of the hardened wheel zone from a ferrite-pearlite mixture with initial grain size of 30-40 μm to a mixture of fine-acicular or structureless martensite with a rosette-type troostite in a ratio of 50:50 %. This produces improvement of mechanical properties (including decrease in friction coefficient in contact of the ridge and the side surface of the rail head) and increase in crack resistance of the wheel material within the plasma hardening zone. Results of

industrial testing with the plasma hardened flanges are show that in all the cases the intensity of wear of the plasma hardened wheel flange was much lower (2.5-3 times), as compared with the untreated wheels [4].

THERMAL STRESS STATE OF WHEELS

At the beginning, the authors of this study attempted to get a deep insight into different aspects of the effect of highly concentrated energy flows (plasma) on the wheel steel material in terms of the processes of surface hardening to extend the life of wheels and tempering of defective wheels prior to reshaping. Further analysis and comparisons showed that for a case of the combined stressed state of the shroud with a cold worked layer the heating of the surface due to friction of brake blocks and rails in blocking of the wheels led to the similar amount of surface defects. It is these defects that may cause the unexpected fracture of the wheel.

The efforts included completion of a package of calculation and experimental studies. Solving the problem of thermal elasticity and thermal ductility was based on a calculation of transient states of thermal stresses through solving the problem of transient thermal conductivity by using the finite difference method. Optimal break-down of a section into triangular finite elements was achieved on the basis of analysis of several variants of the break-down grid. As a result, the section of the shroud (Fig.1a) in zone of the surface microcracks was broken down into 657 elements connected at 365 nodes (Fig.1b)

. Analysis of the results of calculations of thermal, stress and strain states indicates that any type of local heating near the working surface of the shroud leads to thermal stresses, which may exceed the material yield stress (Fig.2). These stresses may cause cracks in embrittlement of the material or a drastic decrease of 2-3 % in ductility. Interference in the shroud leads to tensile stresses formed over its entire section, the level of these stresses being in excess of the material yield stress. In the presence of defects these stresses may cause fracture of the shroud.

INVESTIGATION OF MATERIAL STRUCTURE IN THE WEAKENING ZONE

Network of microcracks looking like a fish scale is formed on the external surface of the wheel (Fig.1a, 3). This zone is an object of our investigations performed by different methods with a purpose to reveal the mechanism of formation of microcracks.

Metallography was conducted using microscopes Neophot-32 and Versamet-2. Microhardness of specimens was determined using the "LECO" microhardness meters at a load on the indenter equal to 245 N. Peculiarities of structure of the wheel material were investigated at a spacing of 0.05 mm. Chemical etching of the specimens was performed in the 4 % HNO₃ solution. The method of quantitative metallography was employed to analyse

variations in grain sizes. Analytical scanning electron microscopy was used to investigate the character of distribution of chemical elements in the zone under consideration, determine chemistry in local regions of phase precipitates and segregations and study the fracture surface. Fractography was used to generate information on the character of fracture, presence of brittle or tough fractures and causes of embrittlement. Direct transmission examination of a fine structure was performed using the JEOL instrument JEM-2000CX.

This examination was aimed at deeper and more detailed analysis of peculiarities of structure, morphology and distribution of different types of finely dispersed phases, their composition, as well as the character of distribution of the crystalline lattice defects and formation of dislocation heterogeneities, including local stress raisers.

Below we describe studies of peculiarities of a structural-phase state of the wheel shroud metal in the roll surface to flange transition zone. This is the zone where the region of surface work hardening formed during operation, combined with surface heating from an external heat source, naturally terminates. It is here that a crack network is formed on the surface (Fig. 3).

Investigations were conducted on groups of specimens to reveal causes of cracking of the subsurface layers of the above zone. Specimens cut in groups are schematically shown in Fig. 4.

The base metal zone (more than 2500 μm deep from the external surface). Base metal (Fig. 5a) has a ferritic-pearlitic microstructure with ferrite fringes precipitating along the grain boundaries. Thickness of these fringes is approximately 1-5 μm . Ferrite grain has a size of approximately 10-35 μm , and size of a pearlite grain is 10-35 μm . Integrated microhardness of structural components is as follows: microhardness of ferrite (H_{μ}^f) is approximately 1300 MPa, and microhardness of pearlite (H_{μ}^p) is approximately 1530-1600 MPa. No cracks were detected in this zone (i.e. in the base metal zone at a distance of about 2500 μm from the surface). Non-metallic inclusions of the sulphide type, having a round shape, were detected (Fig. 5b). This suggests that the initial state of metal containing non-metallic inclusions can lead to additional difficulties in an attempt to provide high service properties of wheelsets.

Direct transmission examinations of a fine structure (Fig. 5c) show that the base metal zone, i.e. to a depth of about 2500 μm , has a structure consisting of clearly defined pearlite and ferrite grains, as well as ferrite fringes. This structure is similar to that of the base metal at a depth of about 5-10000 μm , except that some increase in the dislocation density and decrease in grain size are noted at a depth of about 2500 μm . Transmission examinations revealed also some details of the internal structure of pearlite and ferrite of the base metal.

Thus, the clearly defined contours of extended cementite laminae, having thickness of about 0.015-0.05 μm at thickness of the inter-cementite ferrite layers equal to about 0.13-0.25 μm , are seen in the pearlite grains (Fig. 4c) at the above depth. What is important, and this fact should be given a special emphasis, is that the pearlite grains exhibit no increased dislocation density, much so the dense dislocation clusters. The dislocation distributions observed have a density of about 10^9 cm^{-2} .

As far as structure of the ferrite grains is concerned, these structural components are characterised by a uniform volume distribution of dislocations and formation of a subgranular ($\sim 3.0 \mu\text{m}$) and node-cellular structure (~ 0.5 - $0.7 \mu\text{m}$). The mean dislocation density in ferrite is approximately $8 \cdot 10^9 \text{ cm}^{-2}$.

Ferritic-pearlitic structure of base metal (Fig. 5) in a zone characterised by superposition of external thermal effects on the work hardened material transforms under the surface with a microcrack network (Fig. 3) into a ferrite-carbide mixture with a deformation texture (Fig. 6a).

Here non-metallic inclusions, before being of a globular shape (Fig. 5b), become expanded along the grain deformation line (Fig. 6b). Many microcracks are revealed in the subsurface metal layers (Fig. 6c).

Variations in microstructure through depth of this zone, i.e. from the surface to base metal, have their own peculiar features. At a depth of 0 to 30 μm from the external surface the structure is a ferrite-carbide mixture (slightly etched light region). It contains microcracks oriented at angles of 0 to 30° to the external surface. The length of microcracks in this region is 15-250 μm . The depth at which microcracks are found in the shroud metal ranges from 7 to 35 μm . Thickness of the microcracks is 0.2-3 μm . Distances between the cracks vary from 10 to 500 μm . Here the structure contains finely dispersed carbides in the ferrite matrix and sorbite. Grains are extended at an angle of 12° to the roll surface. This zone is approximately 100-110 μm long. Sizes of the deformed grains are as follows: length is about 10 μm , and width is about 1.0-1.2 μm . The shape factor is 8-10. Microhardness H_μ of this zone is 3410-3210 MPa. Microstructure of the subsurface layer becomes coarser both towards the roll surface (increased work hardening) and towards the working surface of the ridge (increased heat effect).

The angle of inclination of the deformed grains increases with an increase in depth to 230-250 μm . Here it equals 38° to the external surface. Structure of this zone consists of finely dispersed carbides in the ferritic matrix and sorbite. The deformed grains are about 35-30 μm long and 3.5 μm wide. The shape factor is 12-14. Microhardness H_μ of this zone is 2860-2440 MPa.

The angle of inclination of the deformed grains to the external surface is more than 45° at a depth of about 250-450 μm . Structure of this zone also consists of finely dispersed carbides in the ferritic matrix and sorbite.

The deformed grains are about 30-35 μm long and 2.5-4.0 μm wide. The shape factor is 9-14. Microhardness H_{μ} of this zone is 2440 MPa.

The next zone is a transition to base metal. The size of this zone is approximately 3000 μm . No deformation of grains is seen. Structure of this zone consists of ferritic and pearlitic components. The mean size of the ferrite grain is 10 μm and that of the pearlite grain is 7.5-10 μm . Microhardness H_{μ} is about 2320 MPa.

The base metal zone structure consists of ferrite and pearlite. Also troostite rosettes are seen here. Ferrite grain is 10-20 μm in size, and pearlite grain is 35-40 μm . Microhardness H_{μ} of this zone is 2320-2200 MPa.

Chemical analysis (wt. %) of material in the cracking zone (Fig. 6c) showed that the iron content in the bulk of a crack was approximately homogeneous and equal to 98-99 wt. %. There is a scatter of the concentration of manganese, its content inside a crack changing almost two times. The sulphur content varies from hundredths to tenths of a percent. The silicon content inside a crack changes by a factor of about 1.5-2.

At a distance of up to 30 μm from the crack the iron content is also homogeneous and equals 98-99 wt. %. The total manganese content of this region changes by a factor of 1.5. The S and Si contents change approximately two times. Similar concentrations persist also within a wider region (up to 150 μm) around the crack.

Examinations were conducted to reveal non-metallic inclusions and study their composition at a depth of 0-250 μm from the surface. It turned out that at this depth the subsurface layers contained non-metallic inclusions of the sulphide type, having length of about 40-45 μm and thickness of about 2.5-5.0 μm . Chemical analysis showed that the content of Fe inside a sulphide inclusion varied but slightly (from 19.1 to 20.87 %). The Mg content is 50.04-53.34 %. The S content changes not more than by 5 %. The P content is approximately constant. The content of Fe changes not more than by 15 % in the metal zone around a sulphide inclusion (at a distance of up to 70 μm). The Mn content changes by a factor of 4, similar to the S content. The Si content remains almost unchanged.

Therefore, non-metallic inclusions observed at a depth of about 30-70 μm (Fig. 6b) are inclusions of the sulphide type, having a characteristic elongated shape and distributed in parallel to the surface treated.

Non-metallic inclusions of the sulphide type at a depth of 1200-2300 μm from the surface (Fig. 5b) have a composition similar to that of non-metallic inclusions of the sulphide type shown in Fig. 5b. However, their morphology changes, resulting in a globular shape.

Examinations of the character of fracture (Fig. 7) show that the zone of about 100 μm contains the brittle cleavage regions. Analysis of the cleavage surface composition indicates that brittle fracture in this case is related to the presence of extended non-metallic inclusions, as well as to the structure gradient zones.

Therefore, the above-said allows a conclusion that one of the causes of propagation of cracks in the subsurface layers of the wheel shroud metal is formation of expanded elongated non-metallic inclusions of the sulphide type, oriented in parallel to the external surface. This relationship is most evident in fractographic examinations. Structure of metal is also related to cracking. Thus, as seen in the brittle fracture zones revealed by examination of fractures, the brittle cleavage regions propagate along the coarse laminae into pearlite grains, which is indicative of an unfavourable effect of structure of a coarse-laminated pearlite on mechanical properties of metal (and susceptibility of the above types of structural components to cracking).

However, the most intricate structural details, which are impossible to reveal by optical metallography and scanning electron microscopy, can be revealed by direct transmission examination of a fine structure.

Examinations of a fine structure at depth δ equal to about 100 μm from the external surface (cracking zone) made it possible to reveal structural factors which promote formation of cracks. Firstly, the examinations showed non-uniformity and a gradient character of structure with components characteristic of the base metal, i.e. ferrite and pearlite grains. Note that optical examinations failed to reveal the transient structure details in this zone 0-250 μm deep.

Secondly, traces of the temperature treatment effect on structure of cementite laminae in pearlite can be easily seen. The cementite laminae, although they retain their initial (like in base metal) orientation, exhibit obvious degradation, leading to breakdown of a monolithic nature of laminated cementite. Laminae of pearlitic cementite transform into a structure consisting of clusters of dispersed particles of carbides, arranged compactly in a direction of the dissolved laminae of the initially monolithic laminated cementite. Structures of this type and their morphology are indicative of the fact that at a depth of about 100 μm from the surface the structure is transient, exhibiting traces of morphological transformations caused by the temperature effect of surface treatment. However, the general orientation of structural elements (orientation of pearlitic cementite in particular) and presence of characteristic phases (ferrite and pearlite) remain identical to those seen in the base metal.

Thirdly, transmission examinations of a fine structure showed that metal structure in the above zone had all the indicators of the presence of local and very high internal stresses. This implies a high level of dislocation density in the zone of pearlitic cementite laminae. The dislocation density in these regions amounts to about 10^{11}

cm⁻². The presence of a high level of local internal stresses is proved also by formation of extinction profiles in ferrite grains of small sizes (~ 0.1-1.0 μm), characterised by high curvature angles. The profiles are seen as a rule in the ferrite regions adjoining the stressed pearlite regions. Initiation and propagation of cracks take place mostly in these regions (Fig. 8).

The level of local internal stresses (τ) in the zone of contact of the gradient structures was quantitatively estimated. The estimation was done by calculating the value of τ depending upon the dislocation density (ρ) and presence of extinction bend profiles using the following relationship:

$$\tau = G \cdot b \cdot h \cdot \rho / \pi \cdot (1-\nu) [1]$$

where, for steel of the ferritic-pearlitic grade:

G is the shear modulus equal to 84000 MPa,

b is the Burgers vector equal to $2.5 \cdot 10^{-8}$ cm,

h is the thickness of a foil equal to $2 \cdot 10^{-5}$ cm,

ρ is the dislocation density, and

ν is the Poisson' ratio equal to 0.28

Calculations made on the basis of the above relationship show that local strain ϵ_l grows and amounts to a value of $\gg 40\%$ in the region at a depth of about 100-500 μm from the surface. In addition, in regions with a gradient of the dislocation density ($\rho \sim 10^{11}$ - 10^9 cm⁻²), in the zone with an actual dislocation density of $\rho > 10^{11}$ cm⁻² the value of τ (internal stresses) dramatically increases to a level of approximately $G/12$, which is close to values of theoretical strength of a material.

It should be noted that formation of cracks takes place also in regions where phase precipitates of a globular shape are localised, and along the extended phase precipitates located in the grain boundary regions.

Therefore, the mechanism of initiation of cracks in the case of complex loading of the wheelset shrouds can be understood only on the basis of results of direct transmission examinations of a fine structure. In this connection, it seems reasonable to trace variations in structure of the deformed surface layers in the work hardening to heating transition zone (Fig. 9).

Zone 1. As shown by transmission electron microscopy, the surface layers of metal in this zone are characterised by a fragmentation of structure accompanied by formation of finely dispersed elements, such as blocks, fragments and cells with an increased dislocation density (ρ is of an order of $5 \cdot 10^9 - 10^{10}$ cm⁻²) (Fig. 10).

Here the distribution of the dislocation density is comparatively uniform, without substantial gradients of the dislocation density.

These features of the formed structures (decrease in size of the deformed grains compared with sizes of grains of the base metal, increase in dislocation density) are indicative of the fact that prevailing in this region are the structures caused by preliminary work hardening, whereas the temperature field due to a heat source exerts no significant effect on variations in structure of the preliminarily deformed surface. If redistribution of the crystalline lattice defects does take place (as a result of thermal relief of internal stresses), these processes are almost negligible and occur in very local metal volumes (within blocks and cells). As a result, no structural conditions provoking formation of cracks or other defects must arise in the surface layers of metal, where the deformation structures (uniform fine-grained structure having an increased and uniformly distributed dislocation density) are dominant.

Zone 2. As shown by electron microscopy, to a depth from the surface, in the bulk of metal there are extended banded structures (up to 30-40 μm) characterised by (1) a minimum dislocation density inside the bands and (2) clearly defined inter-band boundaries of a high-angle type. This type of structures evidences that in the deformed surface layers of metal, in which preliminary work hardening resulted in formation of a specific banded structure featuring a high level of internal stresses (which is proved by the presence of a high general dislocation density), thermal relaxation of local surface stresses in the above structures occurs with certain peculiarities. These peculiarities include redistribution of dislocations and decrease in their density during the process of thermal relaxation, resulting from development of the polygonisation processes (without formation of recrystallisation nuclei). In addition, the relaxation covered mostly the internal volumes of the deformation bands. As seen, in a certain temperature range the level of the temperature effect is sufficient to activate the relaxation processes by the polygonization mechanism and insufficient to cause development of the relaxation processes by the recrystallisation mechanism. Such temperature conditions do not change structure of the inter-band boundaries. Changes occur primarily in the bulk of the bands.

Therefore, redistribution of dislocations during temperature relaxation occurs in the internal volumes of the bands with no involvement of the inter-band boundaries.

As a result, the clearly defined extended banded structures with elements dramatically differing in the dislocation density are formed in the above surface region. Some of them are characterised by a minimum dislocation density. These are the internal volumes of the bands. And some are characterised by a persisting high level of dislocations. These are the clearly defined inter-band high-angle boundaries. Therefore, the distinct

structures differing in the dislocation density gradient (internal volume – band boundaries) are formed along the extended banded structures during the relaxation processes occurring by the polygonisation mechanism.

In this case it is necessary to take into account orientation (path) of the banded structures. Note that direction of the bands reflects direction of the deformation texture caused by preliminary surface work hardening. In the immediate vicinity to the surface the deformation direction is approximately parallel to the specimen surface ($\angle \varepsilon \sim 0^\circ$). Value of the angle (\angle) of texture changes from 12 to 90° relative to the external surface with increase in distance from the surface to base metal. That is, the bands change orientation they acquired as a result of preliminary work hardening from parallel to almost normal to it. This involves a gradual turn to 90° with distance to the depth of metal (to about 200 μm). Examinations of thin foils showed that transient structures in finite regions (from deformed to non-deformed at a depth of about 200 μm) were of the type of specific spiral-shaped formations (Fig. 11).

It is this zone of a drastic transition and turn of the deformation textures that should exhibit dramatic changes in internal stresses, i.e. from tensile to compressive ones. The latter probably promotes formation of cracks and separation of surface metal layers (formation of the so-called fish scale).

It is likely that the temperature field in this region (this temperature corresponds to the polygonisation temperature) enhances the effect of metal texturing along the extended deformation bands, which is caused by the formed dislocation density gradient between the dislocation density in the bulk and that at the boundaries of the bands. The latter may lead to a more distinct manifestation of reorientation of metal texture from the subsurface deformation region to base (non-deformed) metal.

Zone 3. Examinations by the TEM method showed that structure from the surface to the non-deformed metal layer (base metal) was finely dispersed, with grains characterised by a chaotic orientation. This is indicative of the fact that relaxation of banded structures in metal under the effect of the temperature field occurred mostly by the recrystallisation mechanism, involving formation and growth of recrystallisation nuclei over the entire volume of the bands, including the inter-band boundaries. New recrystallised grains have a dispersed size ($d \sim 0.2\text{-}0.3 \mu\text{m}$) and differing orientation. Such cardinal changes in banded structures are indicative of the almost complete disintegration of structure of the deformation bands and their directed orientation.

This type of the fine-grained and chaotically disoriented structure (Fig. 12) characterised by a comparatively uniform distribution of the dislocation density and absence of local internal stress raisers is favourable for ensuring high mechanical properties.

CONCLUSIONS

1. Phenomenon of loss in strength of the wheel shroud material under the combined effect of service and technology factors was detected.
2. Mechanism of initiation and propagation of surface microcracks which may lead to fracture of the shroud was studied.
3. Recommendations for elimination of dangerous weakening of the wheel material both during operation and in heat treatment were worked out.

References

1. S.Petrov, A.Saakov, Combustion product plasma in surface engineering, TOPAS, Kiev, 2000, p. 265
2. S.Petrov, A.Saakov, Plasma surface hardening of wheelsets, in: T.S.Sudarshan (Ed.), Surface Modification Technologies, IOM Communications Ltd., 1, Carlton House Terrace London SW1Y 5DB, U.K., pp. 516 – 525, 1998.
3. S.Petrov, A.Saakov, Microstructural peculiarities of the steel surface layers treated with a plasma, Advances in special electrometallurgy 1 (1998) 74-80
4. S.Petrov, A.Saakov, Technology and equipment for plasma surface hardening of heavy-duty parts, Materials and manufacturing processes 17(3) (2002) 363-378

List of figure captions

1. Section of the shroud

a – surface microcracks, b – breaking down of the wheel shroud into finite elements

2. Variation of temperature (*a*), thermal stresses (*b*), and strains (*c*, *d*) at different points of the tire in the course of quenching.

3. A network of cracks

4. Schematic of cutting specimens in groups

5. Base metal structure

a) ferritic-pearlitic structure, b) non-metallic inclusions, c) fine pearlitic structure

6. Ferrite-carbide mixture with

a deformation texture (*a*), expanded non-metallic inclusion (*b*) and surface microcrack (*c*)

7. Fractography of the character of fracture

8. Path of a crack in the zone of gradient structures containing inclusions

9. Schematic of cutting of specimens.

1 – zone of dominant work hardening, 2 – zone of the combined work hardening and heating effect, 3 – zone of dominant heating

10. Fragmentation of structure in the dominant work hardening zone

11. Spiral-shaped formations in the combined work hardening and heating zone

12. Fine-grained structure containing no stress raisers in the dominant heating zone

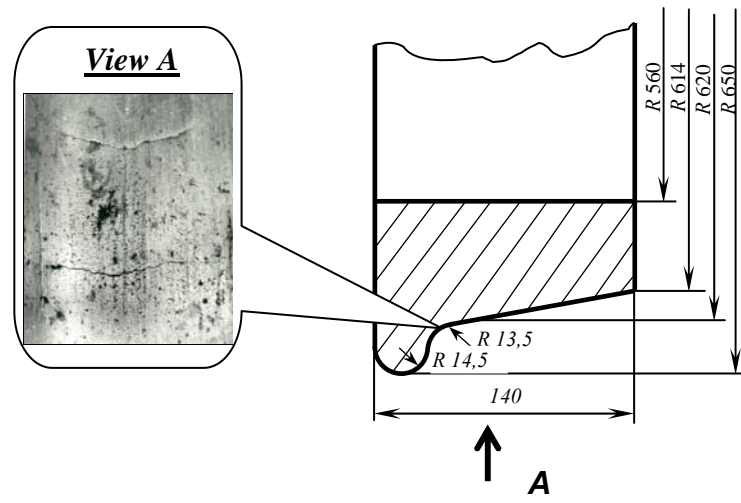


Fig. 1.a

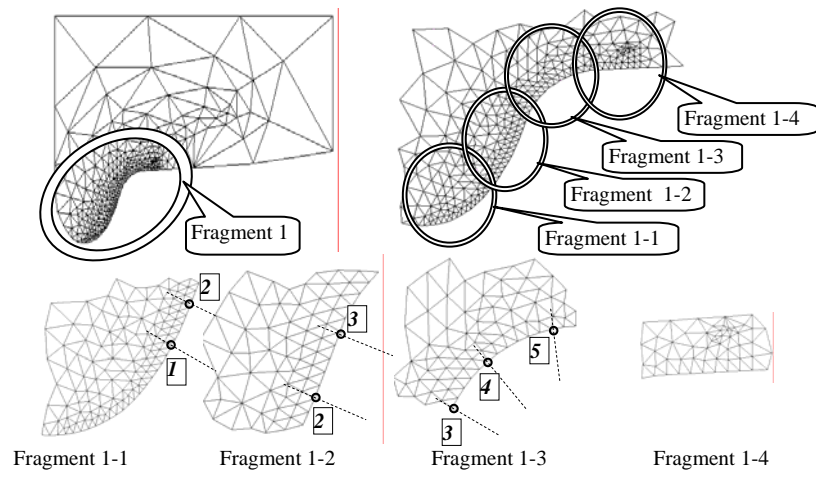


Fig.1b

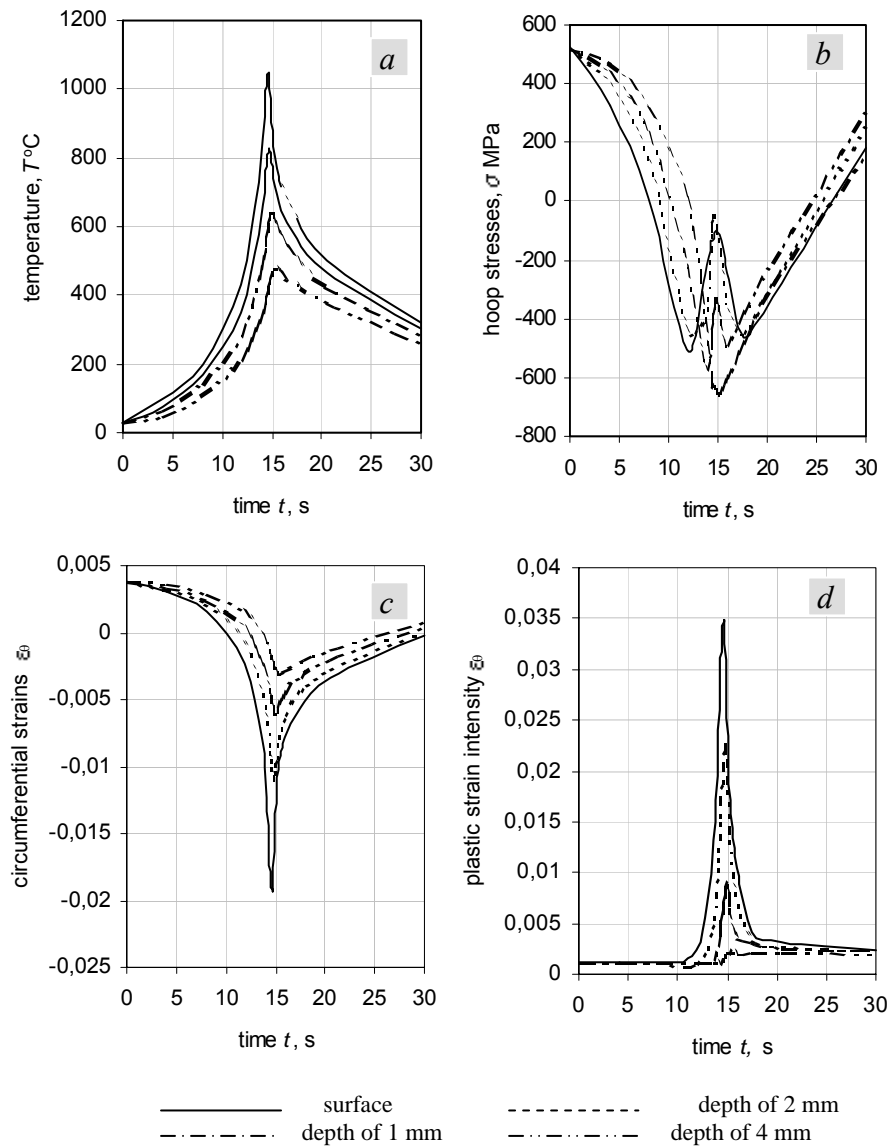


Fig.2

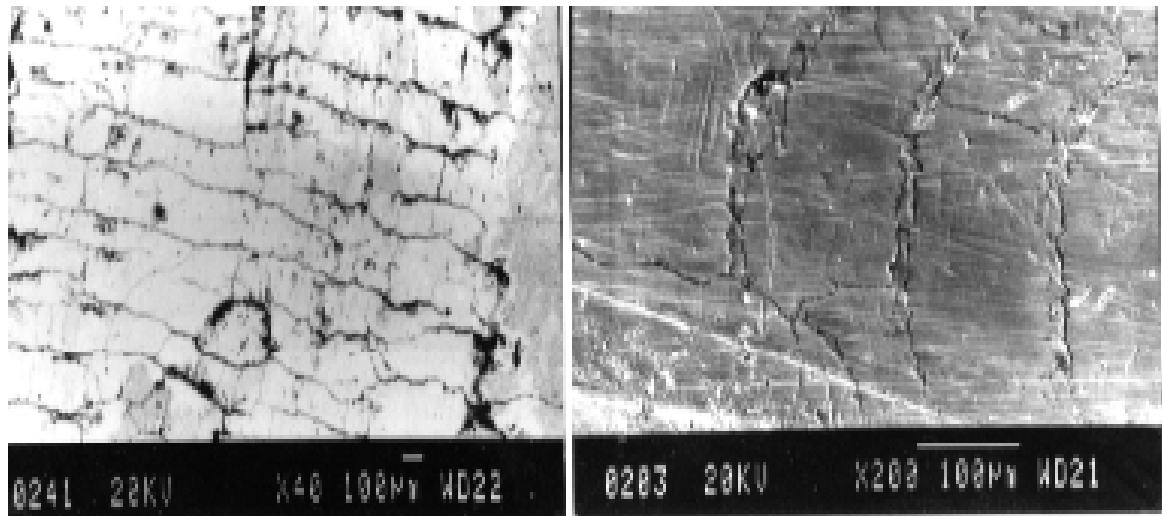


Fig.3

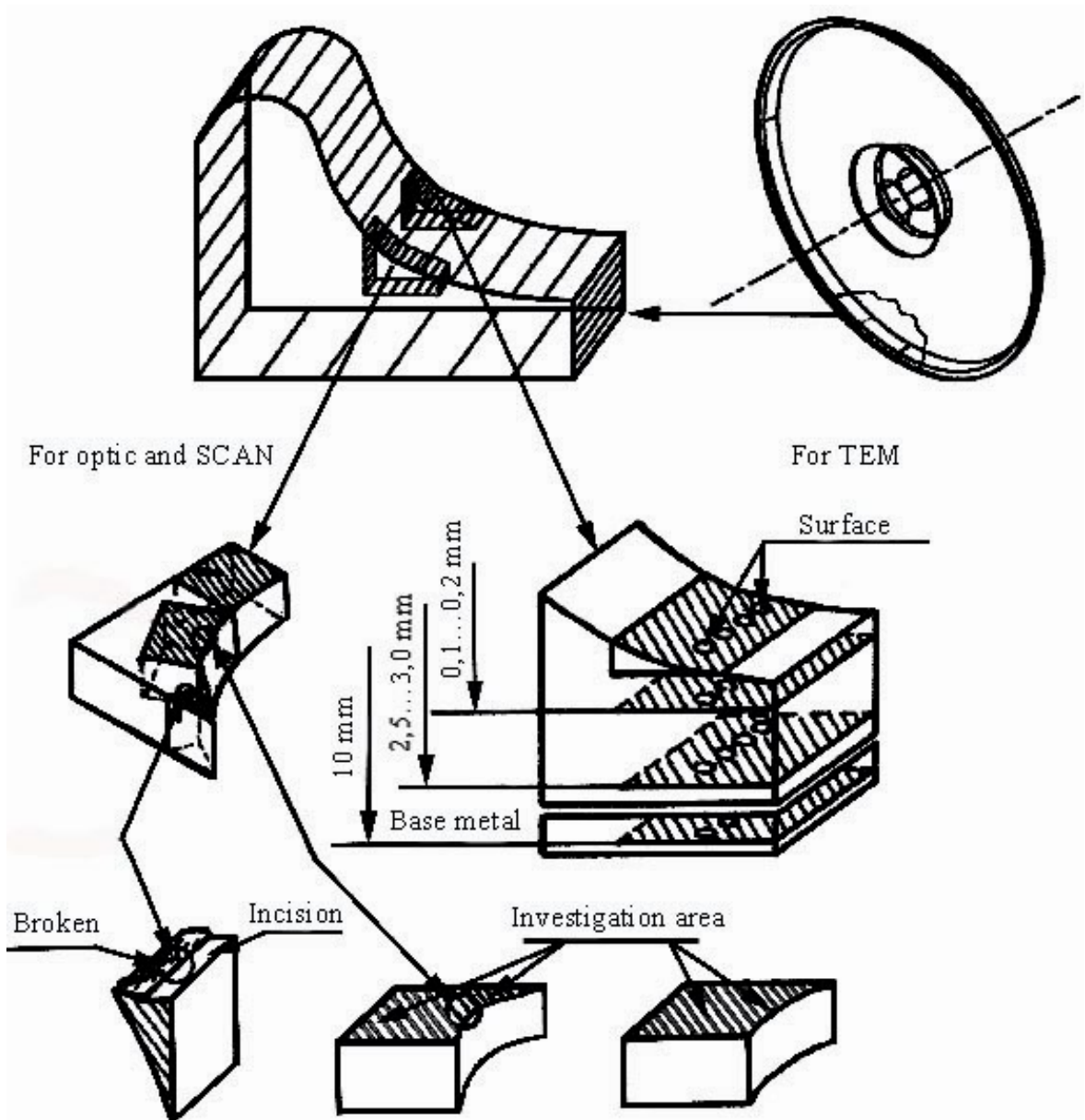
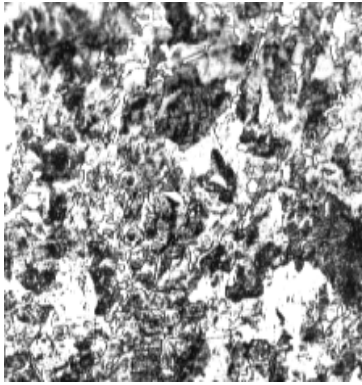
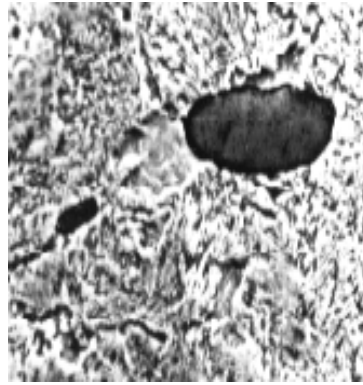


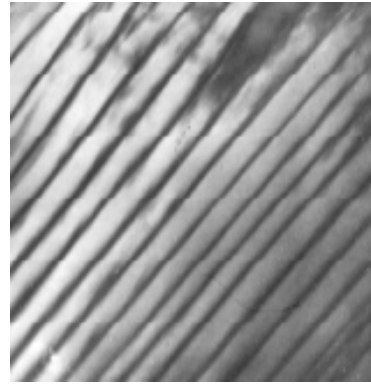
Fig.4



a) $\times 320$

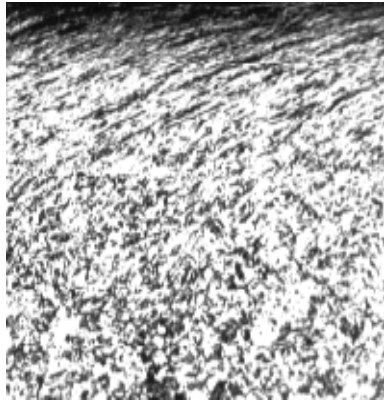


b) $\times 1310$

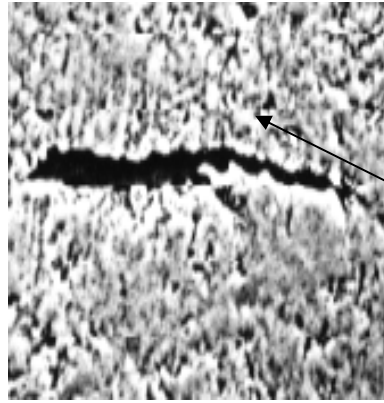


c) $\times 30000$

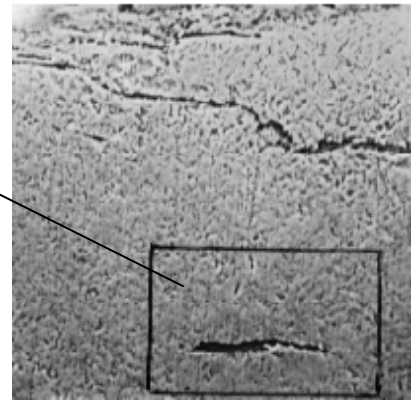
Fig.5



a) $\times 160$

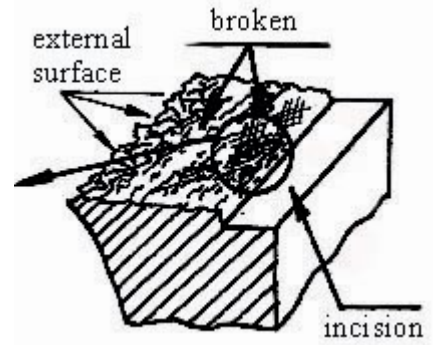
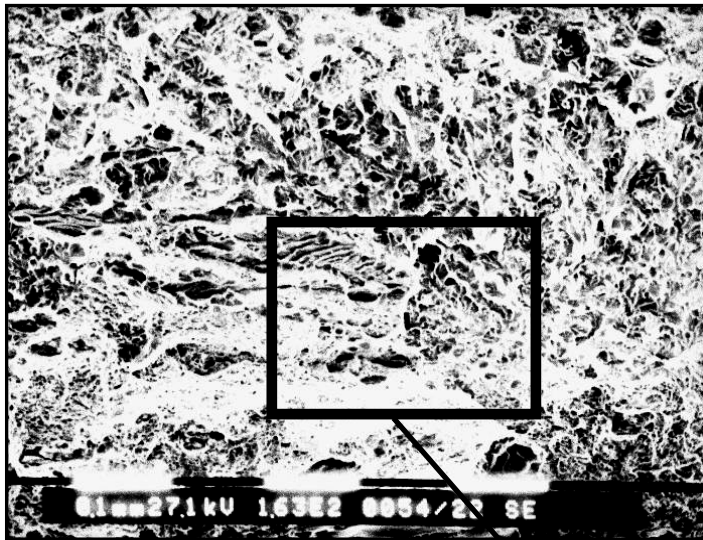


b) $\times 1310$



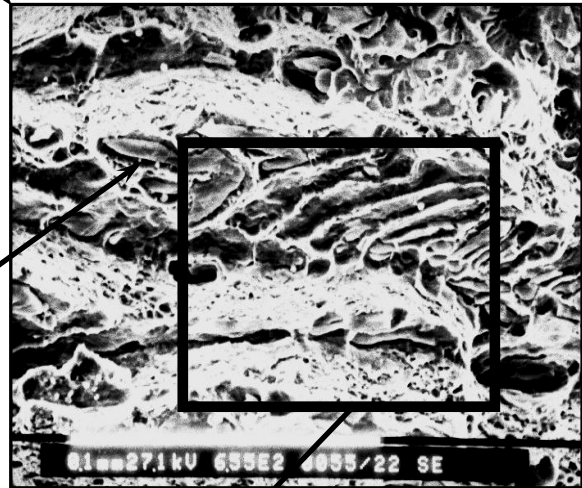
c) $\times 400$

Fig.6



a **x 163**

~30%Fe; ~29%Mn; ~39%S



~10%Fe; ~47%Mn; ~41%S

b **x 655**



B

x 1310

Fig.7



x 15000

Fig.8

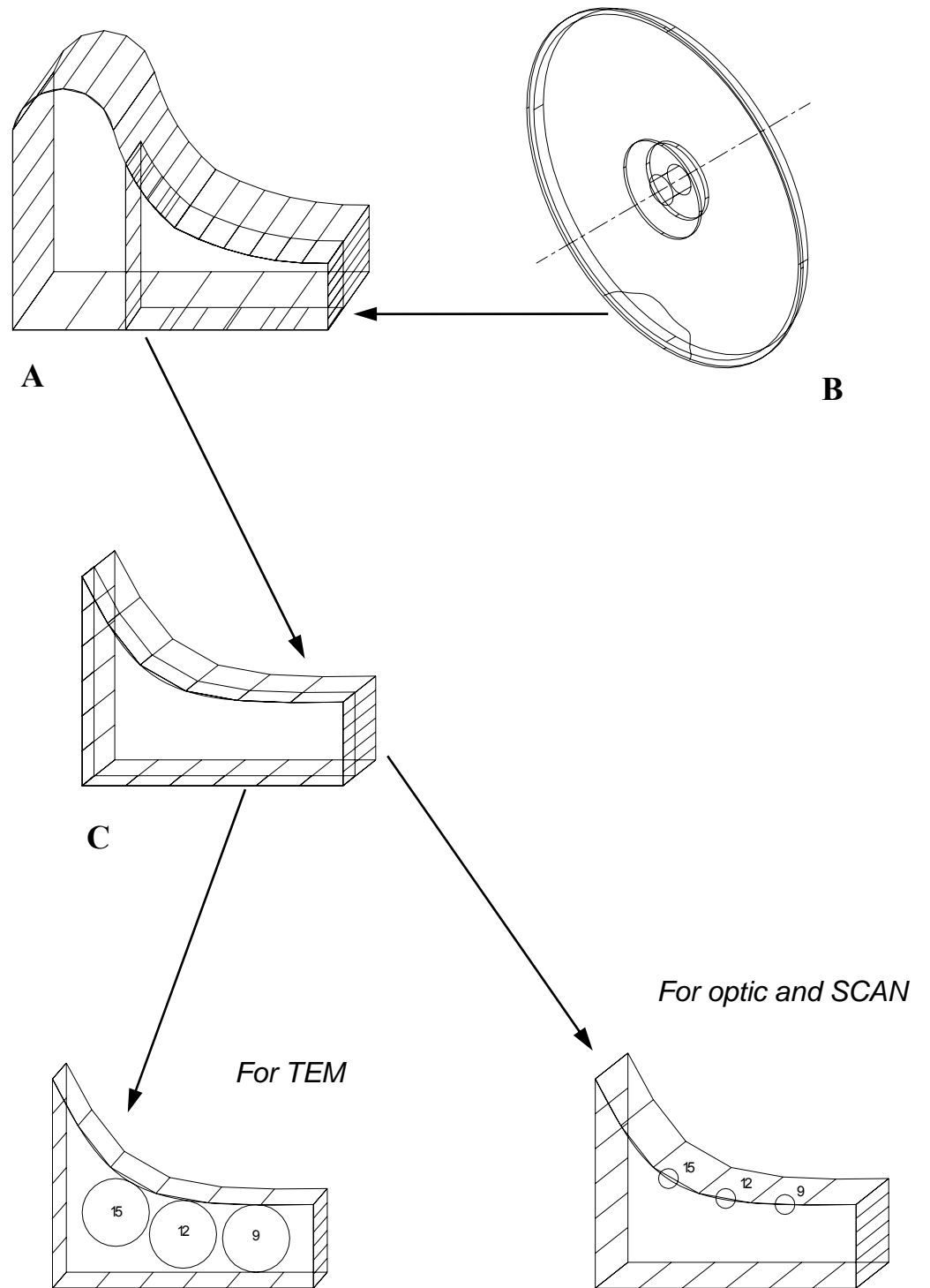


Fig.9



Fig.10

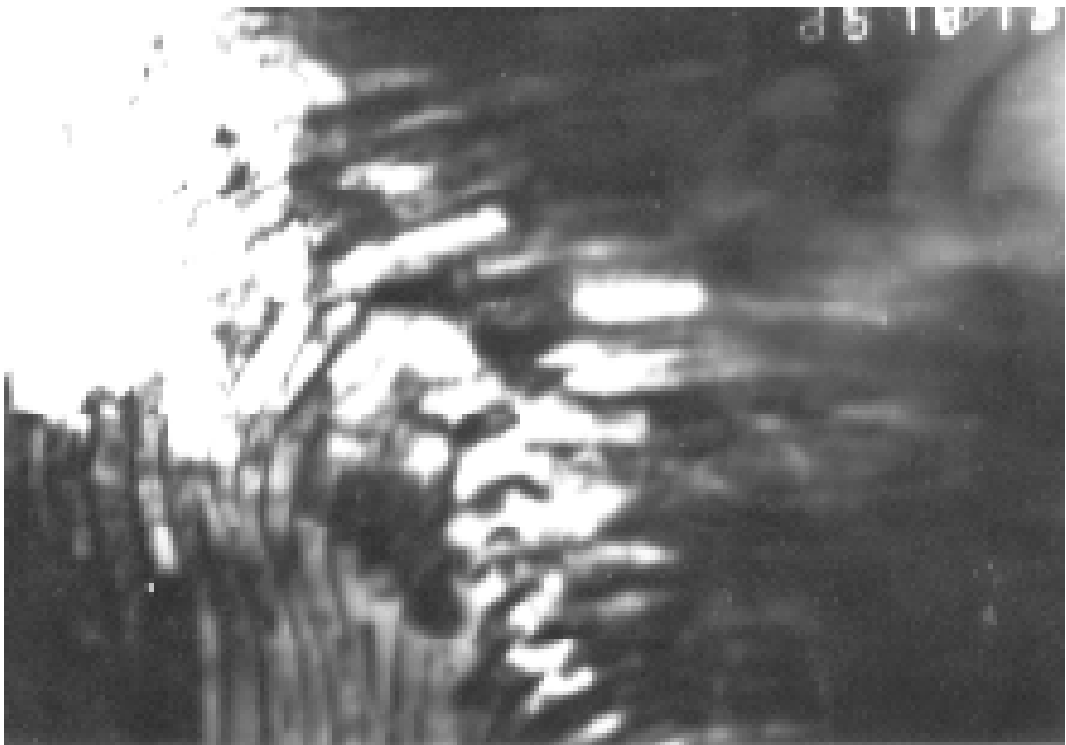


Fig.11

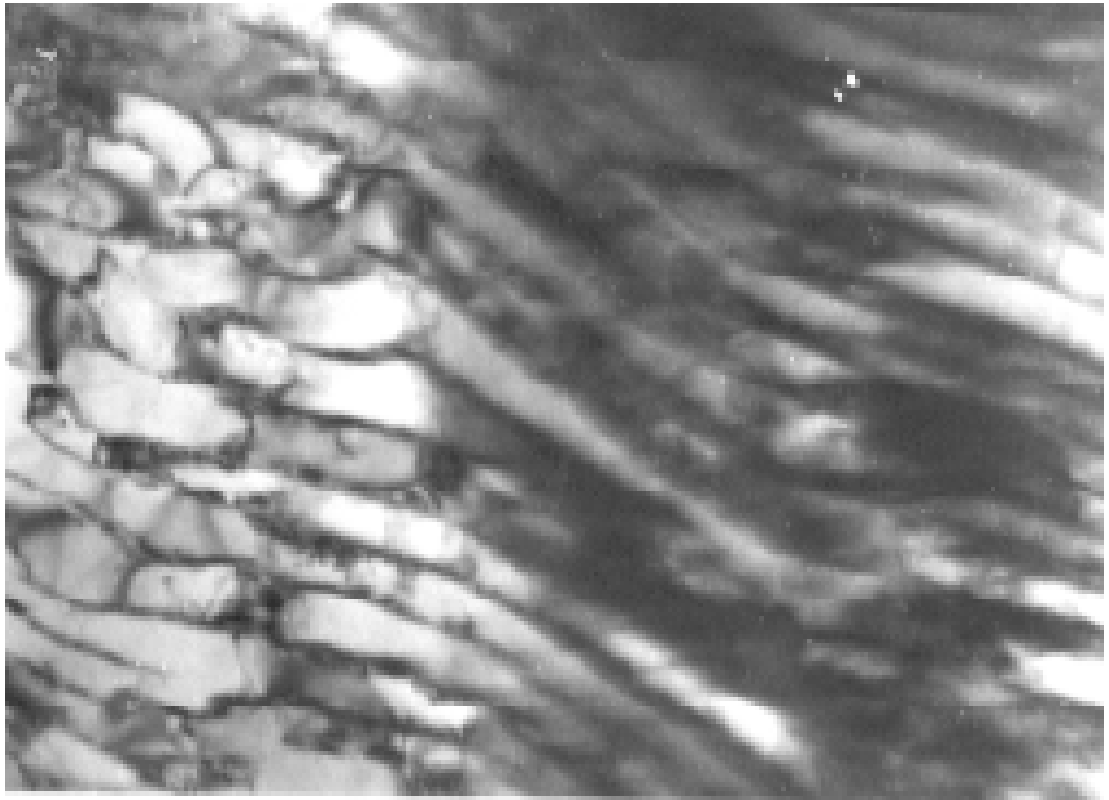


Fig.12

